View metadata, citation and similar papers at core.ac.uk
brought to you by CORE
provided by NASA Technical Reports Server

FEASIBILITY OF ACTIVE FEEDBACK CONTROL OF ROTORDYNAMIC INSTABILITY*

James W. Moore, David W. Lewis, and John Heinzman
University of Virginia
Charlottesville, Virginia 22903

SUMMARY

This paper discusses some of the considerations involved in the use of feedback control as a means of eliminating or alleviating rotordynamic instability. A simple model of a mass on a flexible shaft is used to illustrate the application of feedback control concepts. A description is given of a system now being assembled at the University of Virginia which uses feedback control to support the shaft bearings.

INTRODUCTION

The feasibility of using active feedback control of rotor dynamics by the active control of some or all of the forces in the bearing support system is the subject of research just started at the University of Virginia. If such an approach is feasible, or even partially so, many benefits could accrue to those now having problems of rotordynamic instability.

To study this approach a rotor system using control concepts is now being assembled. It consists of a flexible shaft mounted horizontally in ball bearings at the ends and having provisions for mounting one to three masses. The bearings are each supported by two high-fidelity speaker motors which have a linear range in excess of any expected transients. These motors are mounted at ninety degrees to each other. Induction-type proximity sensors are used to sense shaft position at the bearings and at the central mass. The position signals are then input to the control system, which supplies gain and compensation for the servoamplifiers driving the motors.

The system is designed to use either analog control or computer control of the individual control loops. Initial efforts will use relatively simple control algorithms, but ultimately it is expected that the system will have aspects of pattern recognition and will be adaptive to running speed and to other system parameters.

To illustrate some of the potential benefits of using feedback control, a simple model is analyzed here from the control standpoint. Parameters for the model are selected to be close to those for a system which was the subject of a doctoral dissertation by Marvin Taylor at the University of Virginia in 1979. This work reported on the active feedback control of a rotating cup containing a steel ball which was free to rotate around the inner periphery of the cup. The cup was mounted on a slender shaft, positioned vertically and supported at

*This work was sponsored in part by the Department of Energy under Contract DE-AC01-79ET 13151.

the upper end only. This study was limited in that motion was sensed and controlled in the plane of unbalance. However, Taylor was able to control not only the vibration amplitude at the critical speed but also the whirl of the ball in the cup.

NOMENCLATURE

$A(s)$	loop gain
a_i	polynomial coefficients
c	shaft damping, N s/cm (lb sec/in)
c_i	support damping, N sec/cm (lb sec/in)
$G(s)$	control transfer function
$G_c(s)$	overall feedback transfer function
j	$(-1)^{1/2}$
K	control gain
k	shaft stiffness, N/cm (lb/in)
k_1	support stiffness, N/cm (lb/in)
L	load disturbance
m	rotor mass, kg (lb sec^2/in)
p_i	control and system poles
r	unbalance position, cm (in.)
s	Laplace variable
u	control signal
Z	displacement of mass center, cm (in.)
Z_1	displacement of bearing center, cm (in.)
z_i	control and system zeros
α	ratio of support stiffness to shaft stiffness
ζ	damping ratio
ϕ_i	phase angles
ω	frequency, rad/sec
ω_r	natural frequency

ILLUSTRATIVE SYSTEM

The system to be modeled and controlled is shown in figure 1. For this study complete symmetry is assumed and the bearings are considered as massless. The springs provide the basic support and the control force is additive at the same point. This allows the system to be considered as being of third order. The equations of motion are

$$c_1 Z_1 + k_1 Z_1 + k(Z_1 - Z) = u \tag{1}$$

$$mZ + cZ + k(Z - Z_1) = L \tag{2}$$

where L represents the loading at the mass due to unbalance and u is the control force to be applied. We take the Laplace transform and solve for transfer functions of Z and Z_1 with input u. The unbalance force we will consider as being a load disturbance.

In addition, the shaft damping is considered as negligible. The transfer functions are

$$Z = \frac{(c_1 s + k + k_1)L + ku}{mc_1\left(s^3 + \frac{k + k_1}{mc_1} s^2 + \frac{k}{m} s + \frac{kk_1}{mc_1}\right)} \tag{3}$$

$$Z_1 = \frac{(ms^2 + k)u + kL}{mc_1\left(s^3 + \frac{k + k_1}{c_1} s^2 + \frac{k}{m} s + \frac{kk_1}{mc_1}\right)} \tag{4}$$

The denominator of both equations will have one real root and a pair of complex roots. Using this fact and noting that we need to separate the load and control effects, we can write

$$Z = \frac{(s + z_1)}{m(s + p_1)(s^2 + a_1 s + a_0)} \left[L + \frac{ku}{c_1(s + z_1)}\right] \tag{5}$$

In this form a block diagram can be drawn. This is shown in figure 2, where control and sensor blocks have also been added. In this instance the sensor is assumed to give position and velocity information.

An actuator, the control motor, is assumed to have the transfer function

$$\frac{p_2}{s + p_2} \tag{6}$$

and the controller is assumed to have the form of a gain and a lead-lag function. Combining these factors results in the overall control transfer function

$$G_c = \frac{-K(s + z_2)(s + z_1)}{(s + p_3)(s + p_1)} \tag{7}$$

Combining this with the system transfer function gives a loop gain A(s), which can be used to plot a root locus, which in turn can be used to select the gain and set the control poles and zeros. This function is

$$A = \frac{K_1(s + z_2)(s + z_3)}{(s + p_1)(s + p_2)(s + p_3)(s^2 + a_1 s + a_0)} \tag{8}$$

As mentioned earlier, the parameters for this system were chosen to be approximately equivalent to Taylor's system. This had $k = 20.8$ lb/in and $\omega_n = 85.5$ rad/sec. A number of systems were considered that have second-order parameters close to these. These are listed in table I. Here the entering point is the first column, which is the ratio of support stiffness to shaft stiffness. The second column is the support damping. For each pair of values of these parameters the real pole and zero, the complex poles, and the quadratic coefficients are listed. The parameters chosen for this study are in the row marked with an asterisk.

Root loci of this system for two different values of the control zero are given in figure 3. Also, taking advantage of the vertical symmetry of root locus plots, the lower half plane shows a locus of the system complex poles for a spring rate ratio of 1 and a variable damping factor. The point on the locus for c_1 equals 0.5 is marked with an x, the standard open-loop pole symbol. Its complex conjugate is used in the upper half plane as the starting point for the root loci.

Considering these loci, the solid line is the complex locus with the system motor pole at -200 and a zero at -1. The control compensator pole is at -400 and its zero is at -100.

The dashed line represents the same system except that the compensator zero is moved to -40. The effect is to move the complex locus farther to the left of the imaginary axis. In addition, a new complex locus appears near the real axis.

A root locus is a plot of all possible roots of the closed-loop system with K as the variable parameter. Thus the effect of closing the control loop is very apparent in this case. The principal effect is that the original system poles are eliminated and a new set of poles are established. These poles can be located at any particular points on the branches of the loci by picking a particular value of the control gain K. The poles on the upper complex branch are the ones of particular interest since they will tend to dominate the dynamics of the system. They could be selected for maximum damping or to move them far away from the original system natural frequencies. They represent a quadratic pair in the closed loop system. Considering them only, their damping factor is represented by the arccos ζ, measured from the negative real axis. In figure 3 the maximum ζ lines are shown for both upper branches, and the minimum ζ line is shown for the lower complex branch.

Four values of gain were chosen for calculation of the closed-loop frequency responses of the system. The resulting closed-loop complex poles are re-

presented by the numbered squares on the upper branches. The results are shown in figure 4. Curve 1 is for poles located at point 1 on the solid locus. The resonant peak is about 1.6 at approximately 200 rad/sec. Curve 2 is for the dashed locus with the complex poles having about the same imaginary value as the first case and with the control zero at -40. Curve 3 is from the same locus with the control gain lowered to place the upper complex poles at near maximum ζ. For curve 4 we return to the solid locus and raise the gain to place the complex poles at near the point where the locus crosses the imaginary axis, the point of control loop instability. The response is unbounded for practical purposes at about 270 rad/sec.

EXPERIMENTAL MODEL

The experimental model has already been described and is very similar to the model of figure 1 without the symmetry limitation. Also, the control system almost completely replaces the spring-damper support system and the bearing masses become significant. The analog control system will be of the same form as in the example. All its parameters will be adjustable, and there is provision for making it somewhat adaptive to rotor speed.

The computer control is affected by replacing the control block in figure 2 by a single block Intel 8086 microprocessor and peripherals. Input and output are through appropriate analog-to-digital and digital-to-analog converters. This microprocessor can handle 16-bit words, which allows greater flexibility and precision but which causes it to operate a bit slower than some 8-bit microprocessors. However, preliminary estimates indicate that a computation cycle can be completed about every 10° of rotation of a shaft turning at 6000 rpm. The initial programming of the microprocessor will be of a proportional-plus-rate type with adaptivity to rotor speed and potential for adapting to other parameters.

CONCLUSIONS

The example presented illustrates some of the ability of feedback control to modify the basic characteristics of a rotor system. Potential advantages include the possibility of easily negotiating critical speed ranges; lossless electronic damping; and adaptation to changing load conditions, age, lubricant characteristics, and other factors. In addition, computer control offers the potential of parallel, or even on-line, analysis of system characteristics as a means of recognizing potential trouble and of adapting the control system in an optimum manner.

Yet to be considered in detail are a myriad of the problems of real systems. These include all the present problems, which are well known in rotor dynamics, and adds the problems of control systems. These latter include bandwidth limitations of control components; design of control motors; power and force levels; nonlinearities, particularly signal limiting; observability of appropriate system states; selection of optimum control algorithms; computation speed; and many others. Some recommendations with respect to the feasibility of solutions for some of these problems will be made in the near future. An adequate number of problems will remain for several years of research effort.

The experimental rotor rig was completed by May 20, 1980. It consists of three rotor disks totaling 10 pounds. They are mounted on a 1/2-inch-diameter shaft with a spring rate of 1040 lb/in. The analog control system was operational on May 21, 1980. Initial testing appears to indicate that the performance exceeds expectations. The system was able to run to 6000 rpm without the rotor having been balanced and with no difficulties in negotiating critical speeds.

Efforts in the immediate future will be on the computer control system and on careful testing and evaluations of the system with either analog or digital control. Experimental work will be under the direction of Dr. Ronald Flack, Assistant Professor, Department of Mechanical and Aerospace Engineering, University of Virginia.

TABLE I. - SYSTEM CHARACTERISTICS

α	c_1	Real	Complex	Quadratic coefficients			Zero
0.5	0.1	-296	-8±50j	1	16	2539	-312
	1	-10.6	-10±84j	1	21	7095	-31
	5	-2	-2±85j	1	4.1	7298	-6
1	0.05	-829	-2±60j	1	4.4	3629	-833
	.1	-408	-4.4±61j		8.9	3692	-417
*	.5	-53	-15±74j		31	5695	-84
	1	-22	-10±82j		20	6871	-42
	5	-4	-2±85j		4	7298	-8
	10	-2	-1±86j		2	7311	-4
	20	-1	-.5±86j	↓	1	7310	-2
2	0.1	-621	-2±70j	1	4	4848	-625
	1	-46	-8±80j	1	17	6549	-63
	5	-8	-2±85j	1	4	7280	-12
5	0.1	-1249	-0.5±78j	1	1	6025	-1250
	.5	-245	-2±78j		5	6138	-250
	1	-117	-4±80j		8	6415	-125
	5	-21	-2±85j		4	7229	-25
	10	-10	-1±85j	↓	2	7294	-12
10	0.1	-2084	-0.2±81j	1	0.4	6503	-2084
	.5	-414	-1±81j		2	6530	-416
	1	-205	-2±81j		3	6613	-208
	5	-38	-2±85j		4	7161	-42
	10	-19	-1±85j	↓	2	7270	-21

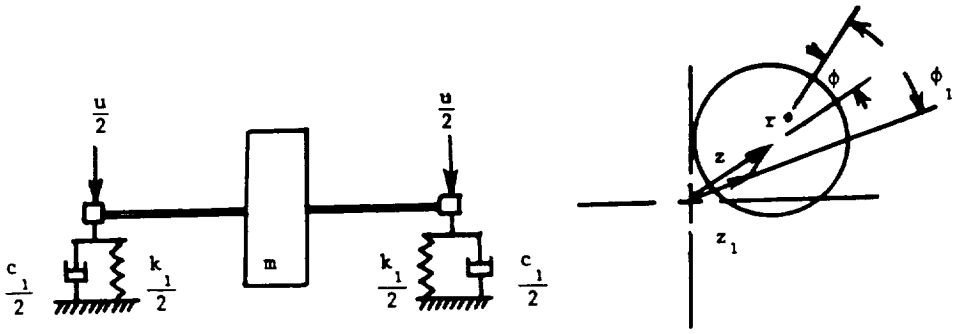

Fig. 1 Physical Model

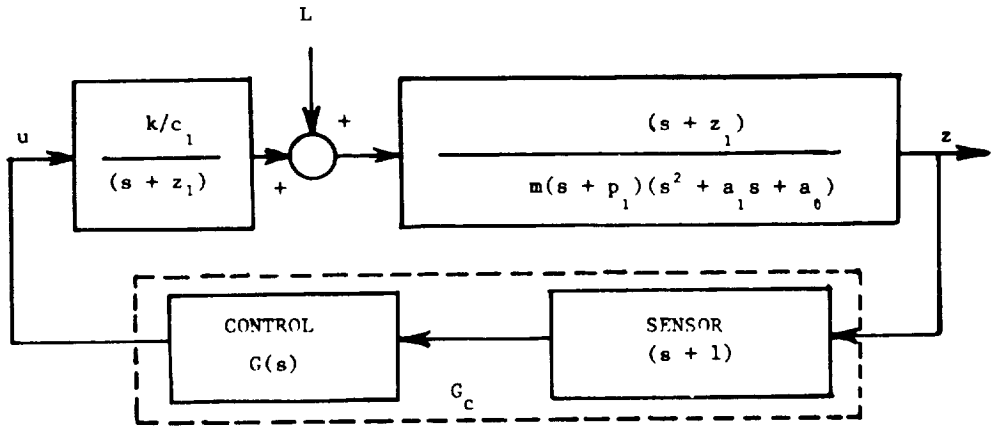

$$G_c(s) = \frac{-K(s + z_2)(s + z_3)}{(s + p_2)(s + p_3)}$$

Fig. 2 Control Model

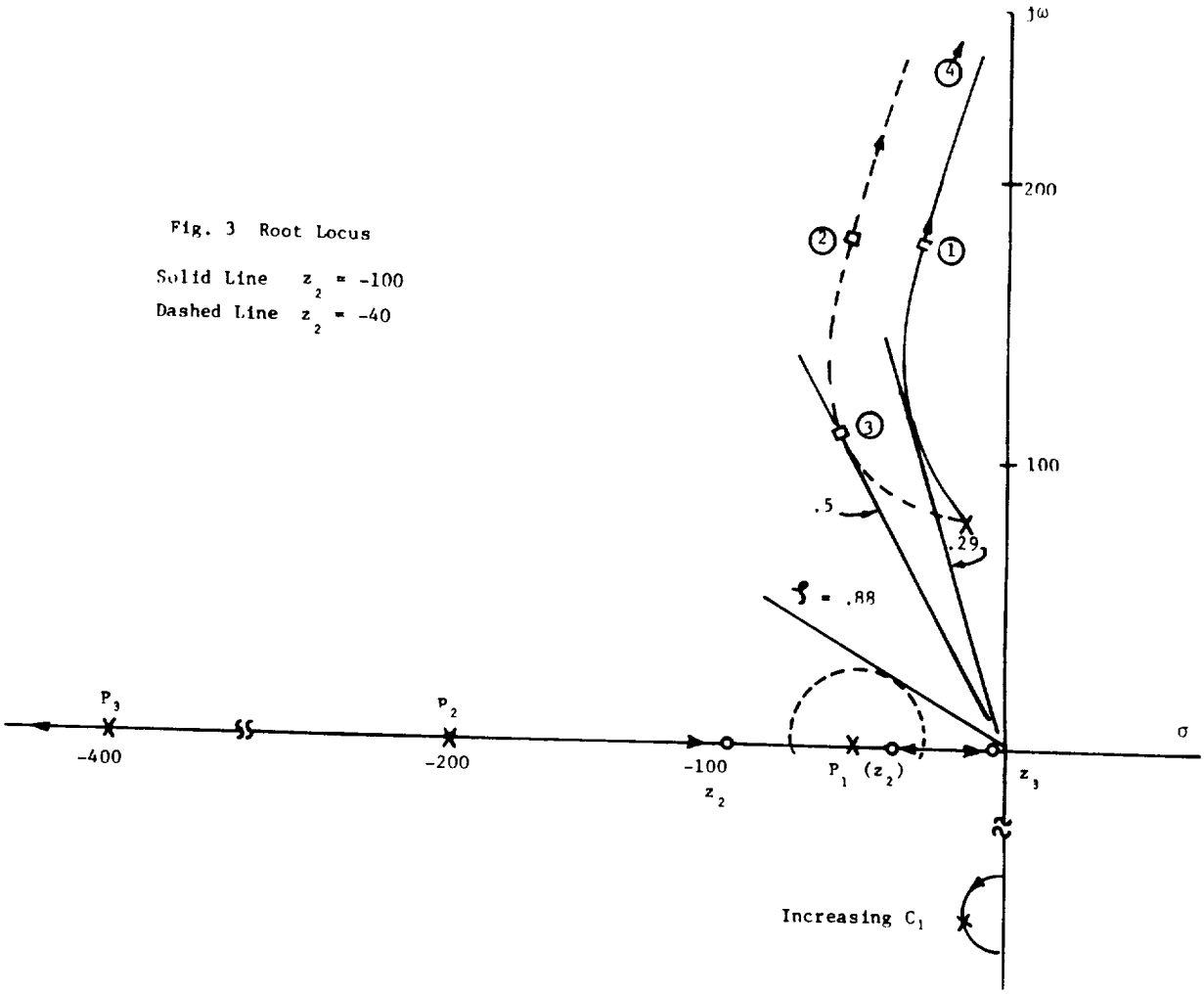

Fig. 3 Root Locus

Solid Line $z_2 = -100$

Dashed Line $z_2 = -40$

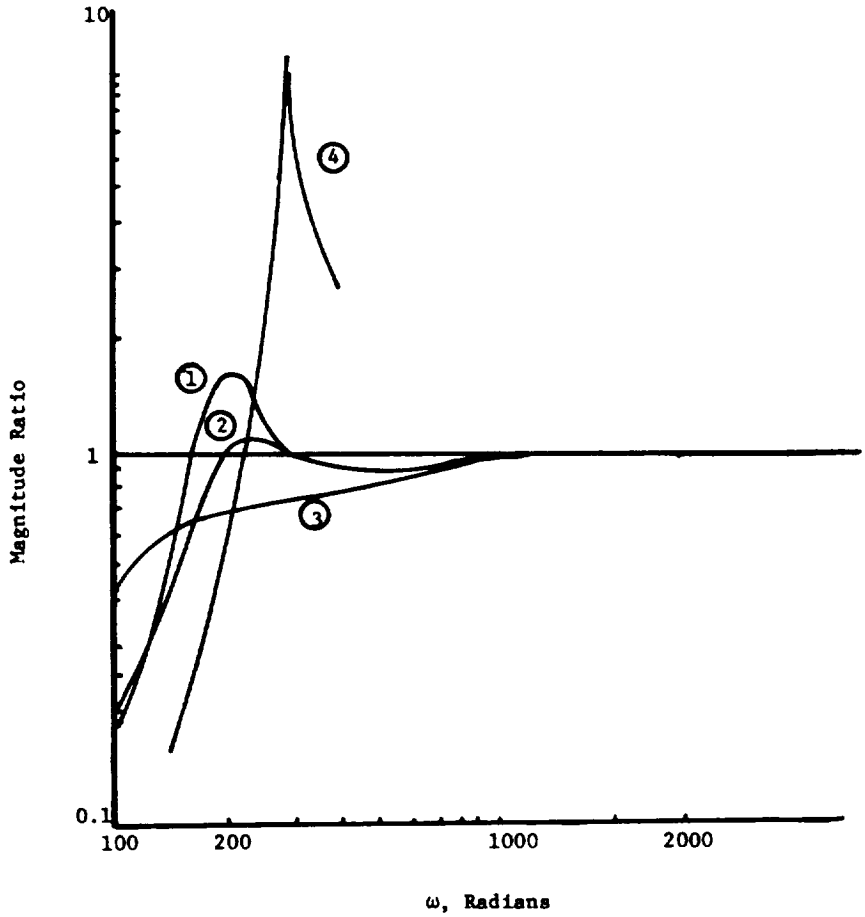

Fig. 4 C. L. Frequency Response